Mechanism for Reversible Electrical Switching of Spin Polarization in $Co/PbZr_{0.2}Ti_{0.8}O_3/La_{0.7}Sr_{0.3}MnO_3$ Tunnel Junctions

M. Imam, N. Stojić,* and N. Binggeli
Abdus Salam International Centre for Theoretical Physics, Strada Costiera 11, Trieste 34151, Italy

(Received 28 March 2018; revised manuscript received 20 July 2018; published 15 January 2019; corrected 22 January 2019)

The possibility of switching the sign of the tunneling electrons' spin polarization by an electric field could introduce dramatic and technologically promising changes in the way spin transport is controlled in spintronic devices. Recently, such switching was observed experimentally in $Co/PbZr_{0.2}Ti_{0.8}O_3$ (PZT)/$La_{0.7}Sr_{0.3}MnO_3$ multiferroic tunnel junctions. Using *ab initio* calculations, we identify a microscopic mechanism that can explain this effect. Following an extensive search, we single out a Co/PZT-interface atomic configuration, including an oxygen-related defect complex, which can account for the experimental spin-polarization switching trend. For this configuration, we find that inversion of the PZT ferroelectric polarization induces drastic reversible changes in the reactivity and chemical binding of the interfacial O with Co. This ferroelectric-controllable reactivity of O leads virtually to an *on-off* switchable O-Co hybridization and a swappable spin polarization in the PZT barrier.

DOI: 10.1103/PhysRevApplied.11.014028

I. INTRODUCTION

Magnetic tunneling junctions (MTJs) with ferroelectric (FE) barriers offer novel ways to control the spin-polarized transport [1]. The insulating barrier is electrically switchable between two stable FE states, which, together with two different magnetization alignments of the electrodes, provides four nonvolatile resistivity states in these multiferroic junctions [2]. Recently, a distinct, exciting property was experimentally observed in the $Co/PbZr_{0.2}Ti_{0.8}O_3$ (PZT)/$La_{0.7}Sr_{0.3}MnO_3$ (LSMO) (001) MTJs at low temperature [3]: the spin polarization of the tunneling electrons could be reversibly inverted by switching of the FE polarization of the PZT barrier, corresponding to a change also of the sign of the tunnel magnetoresistance (TMR). The reversible sign inversion was also reported in subsequent experimental investigations of Co/PZT/LSMO MTJs [4]. In $La_{1-x}Sr_xMnO_3$, $x = 0.3$ was chosen to ensure robust ferromagnetism of LSMO [3]. Namely, the value of x was chosen away from the critical values $\bar{x} = 0.18$ and $\bar{x} = 0.5$ (corresponding to the boundaries of the ferromagnetic metallic phase in the $La_{1-x}Sr_xMnO_3$ bulk phase diagram), for which a FE-induced magnetic phase transition (or reconstruction) of LSMO at the interface was experimentally reported for PZT/$La_{1-\bar{x}}Sr_{\bar{x}}MnO_3$ bilayers [5,6].

The ability to reversibly switch the tunneling carriers' spin polarization with an electric field in the Co/PZT/LSMO MTJ is a big step forward in the field of spin control, which on a more general basis could yield important new opportunities for spintronic applications [7,8]. It is a faster and energetically-more-favorable way of controlling the spin direction of tunneling electrons compared with magnetic switching, which requires large electrical currents [7,8]. Precise knowledge, however, of the microscopic mechanism behind the observed spin-polarization switching effect is lacking and is important for potential optimization, including upgrading the device to room-temperature applications.

As LSMO is a half metal (used as an analyzer of the carriers' spin polarization in the low-temperature experiment [3]), the FE switching of spin polarization in Co/PZT/LSMO MTJs may be expected to occur at the PZT/Co interface [3]. In the limit of a half-metal electrode with a single bulk spin channel for its carriers, neglecting spin-orbit coupling in the ballistic transport, clearly even a magnetic reconstruction at its interface would not change the sign of the TMR or of the carrier's spin polarization. Furthermore, on the basis of the analyzer spin-polarized current, the spin polarization of the tunneling electrons through the PZT barrier changed from negative with respect to the bulk Co majority spin or magnetization when the PZT FE polarization was pointing toward Co to positive when the PZT FE polarization was pointing away from Co.

Most recently, several theoretical first-principles studies [9–12] have tried to account for this reversible electrical switching of spin polarization in the PZT barrier considering ideal defect-free Co/PZT(001) interfaces with either PbO(001) or $Zr_xTi_{1-x}O_2$-layer termination

*nstojic@ictp.it

of PZT and nominal $x = 0.2$ concentration of Zr or also with different x concentration of Zr at the interface. Despite these efforts, the experimentally observed switching has not been reproduced and, more importantly, its underlying mechanism remains unknown. For the PZT FE polarization pointing toward Co, previous calculations could account for the experimental negative spin polarization of the carriers in the barrier [10, 12], which is the natural tunneling trend considering the negative spin polarization, P_s, of the Co electrode, where $P_s = [N_+(E_F) - N_-(E_F)]/[N_+(E_F) + N_-(E_F)]$, E_F is the Fermi energy, and $N_+(E_F)$ is the majority-spin (minority-spin) density of states (DOS) at the Fermi energy. The case of opposite FE polarization, however, requires inversion of the spin polarization in the barrier with respect to the Co electrode (i.e., a Co/PZT-interface *on-off* spin-filtering effect, which is turned *on* when the FE-polarization direction is switched against Co), which has not yet been reproduced theoretically [13].

Experimentally, the Co electrode on PZT is a polycrystalline film [3]. However, a recent Z-contrast transmission-electron-microscopy (TEM) study indicated that the first Co monolayer on the $Zr_xTi_{1-x}O_2$-terminated PZT may be pseudomorphic or have the same lateral periodicity as PZT, at least on the scale of some tens of nanometers laterally [4]. The exact local structural arrangements and chemical composition at the interface are not available, however, from the experiment. On the other hand, the presence of oxygen defects, and in particular of oxygen vacancies, is common for perovskite oxides and at metal/oxide interfaces, and has been reported also for PZT and at PZT/metal interfaces [14–18].

In this study, using first-principles density-functional calculations, we identify a possible mechanism explaining the observed electrical switching of spin polarization. To achieve this, we perform an extended screening of interface configurations, including various types of defects at the PZT/Co interface (intermixing, extra atoms, vacancies, and layer substitution) and their variations. Of all the types of configurations considered, only one reproduces the experimentally observed spin-polarization switching. This configuration is characterized by the presence of a PZT-interface defect complex consisting of an oxygen vacancy and oxygen interstitial pair, with the vacancy in the $Zr_xTi_{1-x}O_2$ interfacial plane and the O atom in the interstitial PZT-Co region. The O defect complex acts as a powerful FE-switchable spin filter. We find that our inverting the PZT FE polarization virtually turns *on* or *off* the reactivity strength of the interfacial O with Co. This FE-controllable reactivity of the interfacial O causes a drastic reversible change in the O-Co distance, a switchable interface hybridization, and a swappable spin polarization.

II. COMPUTATIONAL METHOD

All the structural and electronic properties are studied in the plane-wave pseudopotential formalism of density-functional theory as implemented in the PWscf package of the Quantum ESPRESSO distribution [19]. The calculations are performed within the generalized-gradient approximation with the Perdew-Burke-Ernzerhof parametrization for electronic exchange and correlation. We use scalar-relativistic ultrasoft pseudopotentials [20] including the nonlinear core correction to the exchange-correlation potential [21]. Alloying is treated with the virtual-crystal approximation for Ti and Zr atoms (hereafter called "TZ") in PZT [12], which was previously shown to yield values of structural parameters and dynamical effective charges in complete agreement with the calculations explicitly including the Ti and Zr atoms [22].

For our interface calculations we use slab geometries in a supercell. As we are investigating a magnetoelectric effect at the Co/PZT interface, we include only the PZT semiconductor and Co electrode in our calculations performed for a Co overlayer on a PZT(001) film. As in the experiment PZT is grown as an epitaxial layer coherently strained on a LSMO(001) film, we incorporate the straining effects of LSMO on PZT, without including the actual LSMO slab. We considered the LSMO slab fully in a previous study of the band alignments in the Co/PZT/LSMO trilayer [12], where we examined the chemically abrupt defect-free TZO_2-terminated Co/PZT(001) interface. Here we use the latter interface as our starting (defect-free) reference configuration. Experimentally [3], the LSMO film was grown on a TiO_2-terminated $SrTiO_3$ substrate. Assuming (for stability reasons) a PbO-TZO_2 bilayer-sequence growth of the PZT film, we thus consider TZO_2-terminated PZT on the Co side, consistent with the Z-contrast transmission-electron-microscopy data [4].

All Co/PZT heterojunctions are modeled with commensurate face-centered-cubic (fcc) Co(001)/PZT(001) (1×1) interface atomic structures. The initial defect-free atomic arrangement at the TZO_2-terminated Co/PZT (1×1) interface is adopted from the lowest-energy structure obtained for a very similar system of $Co/SrTiO_3$ [23], and was also used in our previous study [12]. The Co atoms at the interface with PZT are placed at the same lateral positions as the O atoms within the interfacial TiO_2 layer. The supercell for the initial structure consists of seven PZT perovskite structural units (14 monolayers), seven atomic layers of fcc Co(001), and approximately 30 Å of vacuum separating the periodic images of the slab.

For the in-plane lattice constant of the PZT/Co junction, we use the LSMO pseudo-cubic-lattice constant of 3.88 Å [24]. The compressive strain on the pseudomorphic PZT for this lattice constant is about 1.8% along [100] and [010] relative to our optimized bulk PZT lattice parameter. The tensile strain on Co, due to imposed pseudomorphism, is

8.7% along [100] and [010] relative to the optimized Co fcc structure.

Kinetic energy cutoffs of 35 and 350 Ry are used for the expansion of the wavefunctions and augmented charge density, respectively. We use a Γ-centered $14 \times 14 \times 1$ Monkhorst-Pack k-point mesh. A 0.01-Ry Gaussian smearing of the electronic levels is used to improve the k-space integration convergence. These parameter values are identical to those in our previous study [12] on the defect-free Co/PZT/LSMO trilayer.

We refer to the FE polarization pointing toward Co as the "up" polarization direction ($P_\uparrow$) and to the opposite case as the "down" polarization direction ($P_\downarrow$). To set the polarization ($P_\uparrow/P_\downarrow$), the displacements of the atoms corresponding to the desired bulk FE polarization ($P_\uparrow^{\text{bulk}}/P_\downarrow^{\text{bulk}}$) are fixed to the bulk value with $c/a = 1.09$ in three PZT cells (six monolayers) at the vacuum interface. The rest of the atoms are allowed to relax until the forces converge to less than 10^{-3} Ry/bohr. In this way we recover more than 97% of the PZT bulk FE-polarization displacements for $P_\downarrow$ and more then 81% for $P_\uparrow$ in the relaxed layers starting from the second layer away from the Co/PZT interface [25].

In our analysis, we take into account the fact that the experimental spin-polarization reversal was observed for rather thick barriers (32 Å) [3,4] and consider the limit in which LSMO is a perfect half metal with a single spin channel at (and near) E_F. In this limit, we investigate the presence of a Co/PZT-interface spin-filtering effect (when the FE polarization is switched from $P_\uparrow$ to $P_\downarrow$) on the electronic states of the bilayer around E_F by examining their energy-resolved probability densities [26] $\bar{\rho}_{+(-)}(\varepsilon, z)$ integrated over a small energy window around E_F. The label $+$ $(-)$ stands for majority-spin (minority-spin) states. We evaluate the planar-averaged densities $\bar{\rho}_{+(-)}(\varepsilon, z)$; however, the macroscopic averaged densities $\bar{\bar{\rho}}_{+(-)}(\varepsilon, z)$ [26,27] or the layer-averaged densities $\rho_{+(-)}(\varepsilon, n)$ [28] could have been used as well, yielding the same spin-polarization trends for $\bar{\rho}_+(\varepsilon, z)/\bar{\rho}_-(\varepsilon, z)$. Within the framework of the generalized Julliere model for the TMR of thick barriers [29], and assuming the spin-polarized tunneling transport is dominated by the PZT evanescent states with the largest decay length λ_l (the same for two spin channels in the nonmagnetic PZT barrier [28]; see also Fig. 2), the values $\bar{\bar{\rho}}_{(+,-)}(E_F, z)$, for $z = z_{\text{PZT}}$ well within PZT, are measures of (approximatively proportional to) the averaged generalized transmission probability $T^{+(-)}e^{-2d/\lambda_l}$ [29] across the Co/PZT interface, with $d = z - z_0$ the distance in PZT from the interface position z_0 (see Supplemental Material [30]). The ratio $T^+/T^- \approx \bar{\bar{\rho}}_+(E_F, z_{\text{PZT}})/\bar{\bar{\rho}}_-(E_F, z_{\text{PZT}})$ determines the effective spin polarization P_{eff} of the metal/barrier interface that enters the generalized Julliere model [29] for the TMR of thick barriers (see also Supplemental Material [30]). With a half metal as the second electrode, the resulting TMR trends depend only on the effective spin polarization of the Co/PZT interface.

III. RESULTS AND DISCUSSION

A. Atomic interface configuration

Starting from the abrupt Co/PZT interface, we consider a large number of atomic interface configurations corresponding to different types of defects: atomic intermixing, adatoms, vacancies, and layer substitution. In particular, we consider the effect of exchanged interfacial TZ and Co atoms, of TZ and Co adatoms in both the TZO_2 and the interfacial Co plane, and of an extra O atom in the interfacial Co plane with variations of their in-plane positions. Furthermore, we consider the effect of an interstitial O between the Co and PZT films and the effect of an O vacancy in the interfacial TZO_2 layer, and we also replace the interfacial Co layer by a CoO layer (knowing CoO is a layered antiferromagnet in the bulk) with atomic sites in the (PbO) continuation of the PZT perovskite structure [31]. Overall, the only atomic interface configuration able to reproduce the experimental trend for the spin-polarization switching is shown in Fig. 1 for both FE polarizations and contains an O defect complex. With respect to the abrupt TZO_2-terminated PZT/Co interface, in this configuration, one oxygen ion from the interfacial TZO_2 layer (per PZT 1×1 surface unit in our calculation) is taken away and placed in the interstitial Co-TZO_2 region, with the same lateral coordinates as the TZ atom (see Fig. 1) [32]. This extra (interstitial) O ion can also be seen as a continuation of the PZT bulk structure, but without the accompanying Pb atoms, which, for the bulk structure, should be in the same plane. Overall, this defect configuration represents a stable local energy minimum.

As can be seen from the side views of the interfacial region in Figs. 1(c) and 1(d), the equilibrium atomic geometries for the $P_\uparrow$ and $P_\downarrow$ polarizations are remarkably different: there is a considerable separation between the interstitial O and the interfacial Co plane ($d_{\text{Co-O}} = 1.3$ Å) in the case of $P_\uparrow$ [Fig. 1(c)], whereas for $P_\downarrow$ [Fig. 1(d)] this distance is drastically reduced (to 0.6 Å), so the O atom is almost entering the Co layer. For the FE polarization pointing toward Co ($P^\uparrow$), the TZ atoms in the PZT slab are moving toward Co and the O atoms are moving away from Co. This results in an alternate sequence of long and short O–TZ and TZ–O bonds perpendicular to the interface, yielding a long (2.1-Å) O–TZ bond between the O atom of the PbO layer and the interfacial TZ atom, and a short (1.8-Å) TZ–O bond between the interfacial TZ and the interstitial O [see Fig. 1(c)]. On the other hand, for the FE polarization pointing away from Co ($P_\downarrow$), the O atoms are moving toward Co, while the TZ atoms are moving away from the Co plane [see Fig. 1(d)]. This inverts the sequence of short and long O–TZ and TZ–O bonds, resulting in a short (1.8-Å) bond between the O of the PbO

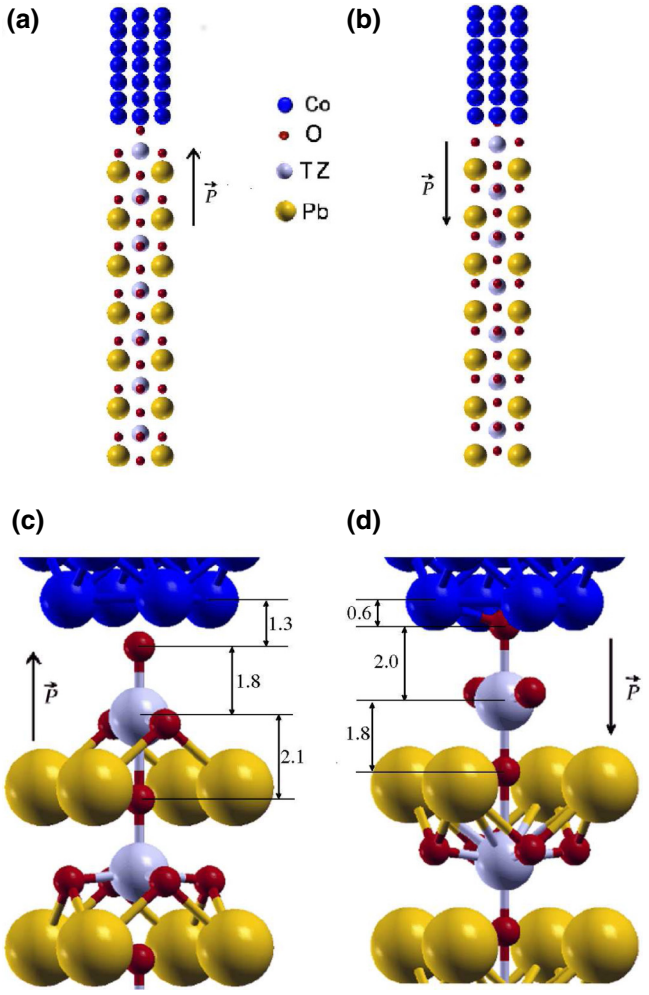

FIG. 1. Side view of the Co/PZT(001) heterojunction in the supercell for the two polarization states with polarization directions $P_\uparrow$ (a) and $P_\downarrow$ (b). With respect to the ideal, chemically abrupt PZT-TZO_2(001)-terminated Co/PZT interface, there is one O atom missing in the interfacial TiO_2 layer, which has been placed closer to the interfacial Co plane. Each Co layer contains two atoms per (1×1) surface cell of PZT. Enlarged side views of the Co/PZT interface areas are shown for $P_\uparrow$ (c) and $P_\downarrow$ (d). TZ denostes the Ti/Zr virtual atom. The equilibrium interfacial Co-O interlayer distance as well as the successive O–TZ and TZ–O distances along the O–TZ–O vertical bonds are indicated in angstroms.

layer and the interfacial TZ, and a long (2.0-Å) bond of the interstitial O with the interfacial TZ [see Fig. 1(d)].

The short (long) bond length of the interstitial O with TZ is indicative of relatively strong (weak) chemical binding of the interstitial O to PZT in the $P_\uparrow$ ($P_\downarrow$) case. We thus attribute the increased (decreased) O-Co separation for $P_\uparrow$ ($P_\downarrow$) to the reduced (enhanced) ability of the O atom to chemically bind to the Co layer, as a consequence of the stronger (weaker) binding to PZT. In other words, switching the polarization ($P_\uparrow/P_\downarrow$) changes the strength of the O–TZ bond (stronger/weaker), which in turn changes the reactivity (enhanced/decreased) of the interstitial O with Co.

The FE-induced switchable reactivity of O is confirmed by separate calculations we perform to evaluate the energy of adsorption/binding of a single Co atom to the interstitial O in the PZT slab (the same slab as in Fig. 1) with all the PZT positions frozen as in the $P_\uparrow$ and $P_\downarrow$ cases. From these calculations we find that in the $P_\downarrow$ case the binding energy is larger by 1 eV than for the opposite polarization. Moreover, by calculating the difference in the binding energy of the full Co slab with PZT for the two polarizations, we similarly find that it is 2 eV larger per PZT (1×1) surface unit (two Co surface atoms) for $P_\downarrow$, confirming a major difference in the strength of the Co-O interaction for $P_\uparrow$ and $P_\downarrow$. This indicates that changing of the FE polarization can actually switch the strength of the interaction between the interstitial O and Co atoms, serving virtually as an *on-off* switch for hybridization. As we will see in the next section, this switchable chemical interaction between O and Co acts as a swappable spin filter, which for the $P_\downarrow$ FE polarization inverts the sign of the spin polarization P_s in the barrier relative to the Co-electrode spin polarization. As we will see, this occurs via reversal of the interstitial O spin polarization.

The presence of the O vacancy in the TZO_2 layer makes the TZ atom more prone to interact with the interstitial O than in the case without the vacancy. In one of our trial configurations without the vacancy and with the interstitial O atom between TZ and the Co layer, the distance, for $P_\downarrow$, between TZ and the interstitial O increased to 2.2 Å and the O-Co distance decreases to 0.2 Å. The interstitial O atom has the desired inverted spin polarization but it fails to couple to the TZ atom in the neighboring layer, which remains non-spin-polarized. The trial configuration consisting of only the O vacancy in the TZO_2 plane is the only one, besides the final one consisting of both the O vacancy and the interstitial O, able to reproduce correctly the spin polarization for $P_\downarrow$ in the barrier. However, it fails to reproduce even the right trend of the spin polarization when the FE polarization is switched to $P_\uparrow$. In other words, the O vacancy strengthens the interaction between the interstitial O atom and the TZ atom, making it possible to propagate the interstitial-O spin polarization to the barrier. For this reason, the interstitial O may be viewed as a "bridge" between the Co layer and the TZ atom.

B. Spin-polarization switching

The change of PZT FE polarization from $P_\uparrow$ to $P_\downarrow$ inverts the spin polarization of the evanescent metal-induced gap states (MIGSs) in the PZT barrier at and near E_F with respect to the spin polarization of the Co electrode (at and near E_F). This is shown spatially for the

MIGSs in Fig. 2, where we present the planar average of the probability density of the spin-polarized states of the junction around E_F integrated in an energy window from -0.2 to 0.2 eV. The probability density is shown across the Co/PZT interface for the two FE polarizations. The aforementioned specific energy window is used just for an accurate k-point convergence of the probability density (given the k grid used for the integration; see Sec. II), but also for smaller windows the result does not change qualitatively [33].

For small bias, the probability density in the barrier, $\rho_{(+,-)}(E_F, z_{\mathrm{PZT}})$, of the stationary states (MIGSs) at E_F (or integrated in a related small energy window), as shown in Fig. 2, is a sound quantity to discuss the trends of the conductance within the generalized Julliere model [30,34]. In the case of the $P_\uparrow$ polarization [Fig. 2(a)], the dominant states are of minority spin polarization in the Co slab and in the PZT barrier. In the $P^\downarrow$ case [Fig. 2(b)], the spin polarization of the dominant states changes across the interface, starting from the minority spin polarization in the Co layer and then switching to the majority spin polarization at one point between the O and TZ atoms. This trend for the switching of the spin polarization from minority (negative) to majority (positive) spin polarization by change of the FE field from $P_\uparrow$ to $P_\downarrow$ is reflected in the TMR ratios from the generalized Julliere model [34] and is consistent with the experimental trend for the tunneling current [3].

For the $P_\uparrow$ case, in Fig. 2(a), one can notice a local enhancement or shoulder in the MIGS probability density at or near the position of the interstitial O, in both the majority channel and the minority channel. This corresponds to the spin-polarized states of the bridge O, as we see later in this section, which for $P_\uparrow$ transmits the minority spin polarization of Co to the MIGSs in the barrier. For the $P_\downarrow$ case, this local feature disappears and a major spin-filtering effect is seen across the interface in Fig. 2(b), when the interstitial O moves to a position very close to Co. The probability density of the minority-spin MIGSs drastically decreases in the PZT barrier, compared with the majority-spin MIGSs, causing a threefold reduction of the minority-spin probability density at the position of TZ relative to the majority-spin states. The evanescent/tunneling states continue to carry the same positive spin polarization deep into the barrier, as can be seen in Fig. 2(b). In the insets in Fig. 2 we also display the layer-resolved DOS within the heterojunction in an energy window including the PZT band gap. This shows that the spin-polarization inversion occurs in an energy region of at least ± 0.5 eV around E_F [35]. Moreover, it can be concluded from Fig. 2 and comparison with the defect-free case [12] that the effect of the defect is very strong on the spin polarization for both FE polarizations and that even a smaller defect concentration would yield the correct spin polarization for $P_\downarrow$ and would, actually, even improve the TMR agreement with experiment [3] for $P_\uparrow$ and $P_\downarrow$ [36].

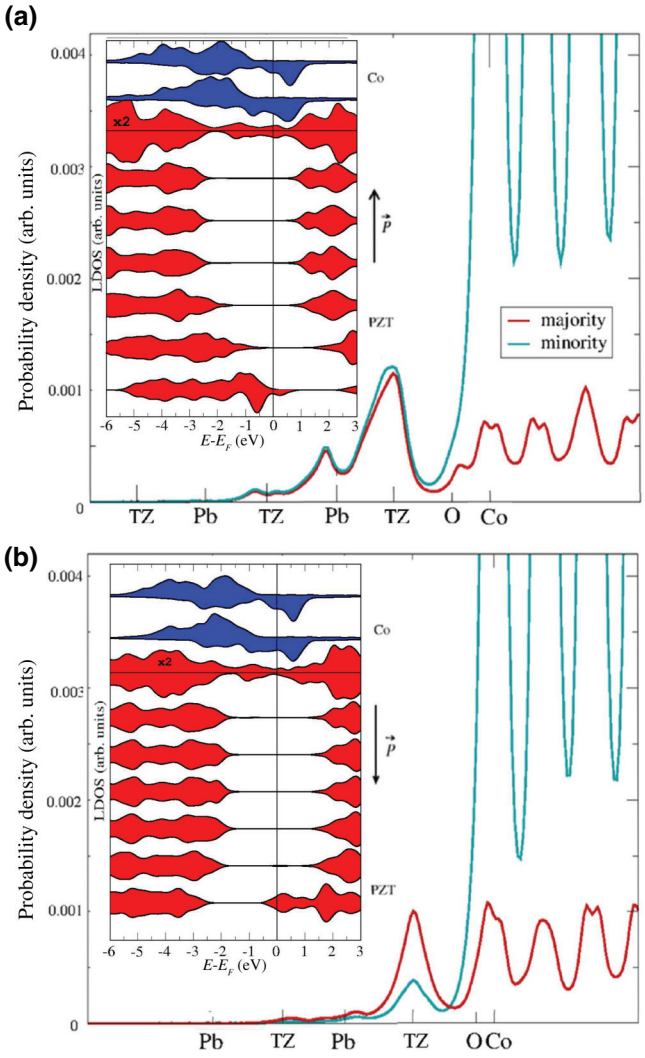

FIG. 2. Planar average of the probability density of the electronic states in the Co/PZT(001) heterojunction, integrated over an energy of ± 0.2 eV around the Fermi energy for (a) $P_\uparrow$ and (b) $P_\downarrow$ polarization, demonstrating the switching of the tunneling-state spin polarization on change of FE polarization (minority spin for $P_\uparrow$ and majority spin for $P_\downarrow$). The positions of the PZT layers are indicated by the Pb and TZ atoms and the interstitial O on the horizontal axis. The insets show the spin-polarized layer-resolved DOS (for simplicity, only two Co layers are shown), where the upper (lower) half of each DOS layer represents the majority-spin (minority-spin) states. Each DOS layer in PZT (Co) corresponds to one PbO-TZO_2 bilayer (one Co monolayer).

Comparison of the MIGS probability densities in PZT for $P_\uparrow$ and $P_\downarrow$ in Figs. 2(a) and 2(b) shows that, apart from the sign reversal of the spin polarization, there is also a significant overall decrease (in both channels) of the probability density of the evanescent/tunneling states in the PZT barrier on our changing the FE polarization from $P_\uparrow$ to $P_\downarrow$. This trend is also consistent with the experimental transport behavior [3], showing a substantial decrease (an order

of magnitude or so) in the conductivity when the FE polarization is switched from $P_\uparrow$ to $P_\downarrow$. The overall decrease in the probability density of the PZT barrier states, from $P_\uparrow$ to $P_\downarrow$, in Fig. 2 is due to the change in the position of the Fermi energy at the Co/PZT interface. E_F moves from a position relatively close to the PZT conduction-band edge, for $P_\uparrow$, to a position deeper within the PZT band gap, for $P_\downarrow$ (see the insets in Fig. 2). This change in the position of the Fermi energy at the interface decreases the decay length of the MIGSs at E_F [12] and thus their probability density within the PZT barrier. A similar behavior is present at the defect-free Co/PZT(001) interface, although no spin-polarization reversal occurs in that case [12].

To better understand the origin of the spin-polarization switching, we investigate the effects of the change in the FE polarization direction on the local density of states (LDOS) of the atoms at the interface. In Fig. 3 we plot the LDOS of the interfacial Co, O, (interstitial), and TZ atoms for the two FE polarizations. Figure 3 shows that while for $P_\uparrow$ O adopts the negative spin polarization of Co (i.e., has a larger LDOS at E_F in the minority channel), the change to $P_\downarrow$ switches the O spin polarization to positive, with a larger LDOS at E_F in the majority-spin channel. The sign of the O spin polarization (negative for $P_\uparrow$ and positive for $P_\downarrow$) is then transferred to the LDOS at E_F of the neighboring TZ atom (Fig. 3) and then further to the MIGSs deeper in the PZT barrier, as observed in Fig. 2.

The reversal of the O spin polarization in Fig. 3 can be understood as a consequence of the strong O-Co chemical bonding/interaction, which is established (see Sec. III A) when the FE polarization is switched from $P_\uparrow$ to $P_\downarrow$ (with a striking decrease in the O-Co separation and a drastic increase in the Co-PZT binding energy). The difference between weak and strong O-Co chemical interaction or hybridization, for $P_\uparrow$ and $P_\downarrow$, respectively, is apparent also when we compare the O LDOS in Figs. 3(a) and 3(b), both in the general features of the O p band and in the more-detailed properties of the MIGS LDOS near E_F. In particular, with the strong Co-O interaction turned on (for $P_\downarrow$), the O band overall significantly broadens (by about 1.5 eV), while displaying a strongly increased DOS at the very bottom of the majority-spin and minority-spin O band, as well as the occurrence of a significant exchange splitting (approximately 0.5 eV) between the main feature of the majority-spin and minority-spin band [37].

Furthermore, on examination of the O LDOS in the energy region of the MIGSs in Figs. 3(a) and 3(b) (i.e., within the PZT band-gap range from -2.5 to 1 eV for $P_\uparrow$ and from -2.0 to 1.5 eV for $P_\downarrow$ (see the insets in Fig. 2), one also observes major differences between the $P_\uparrow$ and $P_\downarrow$ cases. For $P_\uparrow$ ($d_{\text{Co-O}} = 1.8$ Å), the O LDOS in the PZT band-gap region mostly reproduces, with attenuated intensities, the Co LDOS features. In particular, in the majority-spin channel, the O MIGS-related p states simply match the tails (on the O side) of the Co low-density

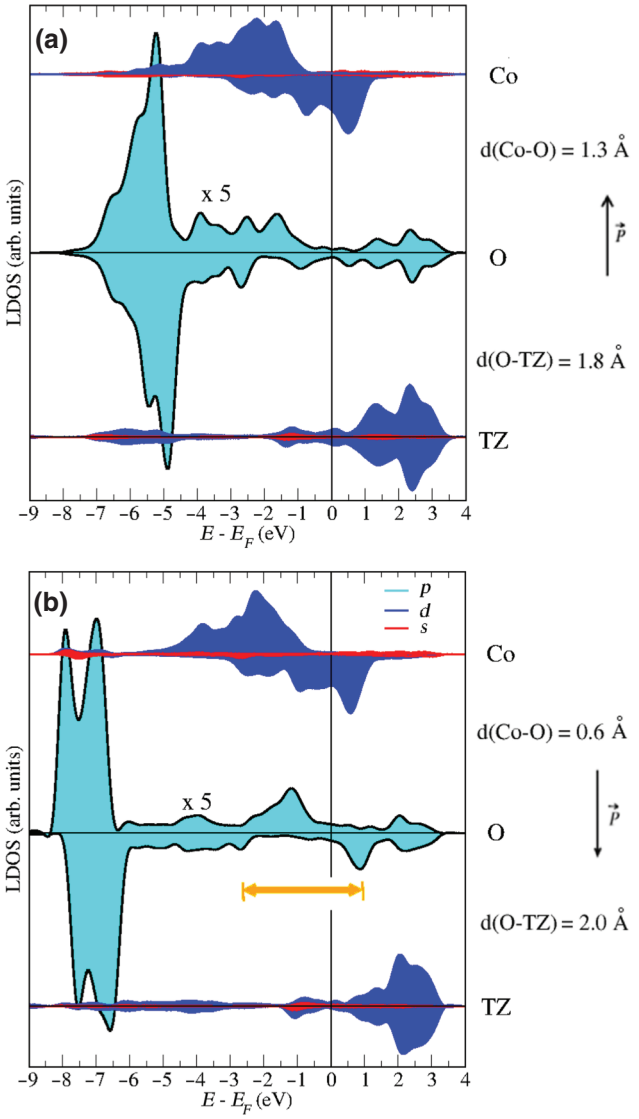

FIG. 3. Spin-resolved local density of states of the interfacial Co, O (bridge O), and TZ atoms in the Co/PZT(001) heterojunction for (a) $P_\uparrow$ and (b) $P_\downarrow$ polarization. To ease the viewing, the LDOS of the bridge O is multiplied by 5. The upper (lower) half of each DOS layer represents the majority-spin (minority-spin) states. The orange arrow denotes the depletion in the LDOS of the O p states.

s states around E_F, leading to a low O LDOS near E_F. Analogously, in the minority-spin channel, the O MIGS-related p states also essentially just match the tails of the high-density Co d states around E_F, resulting in a higher O minority-spin LDOS than majority-spin LDOS around E_F, in Fig. 3(a). This behavior reflects a rather weak Co-O interaction. For $P_\downarrow$ ($d_{\text{Co-O}} = 0.6$ Å), on one hand the closeness of Co and O causes the presence of more MIGSs at the O position, increasing the overall O LDOS within the PZT band gap, especially in the majority-spin

channel. On the other hand, the decreased O-Co separation strongly increases the hybridization between the O p states and the high-density Co d states in the minority-spin channel. This causes a redistribution of the O p states in antiphase with the LDOS of the Co minority-spin d band, resulting in a striking O minority-spin LDOS depletion in the energy region from -2.5 to 0.5 eV, shown in orange in Fig. 3(b). Such behavior, deriving from a strong hybridization, has been observed and analyzed also in other systems, including oxide interfaces and 3d alloys [38,39]. The enhancement of the Co($3d$)-O($2p$) interaction for $P_{\downarrow}$ is thus responsible for the reduction of the O minority-spin LDOS at E_F, which is the reason why the O spin polarization reverts to positive in this case. The strength of the Co-O interaction emerging from the LDOS behavior also confirms the picture of the virtual *on-off* FE switching of the hybridization.

Thus, in our system we show that the spin-polarization switching in the barrier occurs mainly because of the change of reactivity of the interfacial O atom, governed by the FE displacements, which in turn controls the O hybridization with Co and determines the tunneling electrons' spin. This FE-controllable reactivity of the interfacial O is a different dynamical mechanism to reversibly swap the spin polarization by switching the hybridization at the interface in comparison with previously described methods to statically engineer the spin polarization by permanent modifications of the junctions (including changing the barrier material or growing ultrathin interfacial layers) [40,41]. We also note that the mechanism based on the activation of the interface O reactivity that we uncover in this study differs in nature from the interface magnetic-phase-transition mechanisms recently evidenced at some metal/ferroelectric interfaces [5,6,42,43]. The latter account for a FE switching of the transition-metal magnetization at these interfaces, as opposed to the reversal of the spin polarization of the tunneling electrons in the barrier (which is more difficult to achieve and has been observed so far only in Co/PZT-based MTJs) [3,4]. At the same time, the mechanism described here, based on the FE-induced change in the reactivity of O and its ability to *chemically* bind to the Co layer, is different in nature from the electronic mechanism of the FE-induced TMR inversion in Co/polyvinylidene fluoride/O/Co [44], where the effect arises from a change in the screening of the polarization charges.

We emphasize that for experimental realizations of the ferroelectric spin-polarization switching, based on our proposed mechanism, the choice of the second electrode in the multiferroic tunnel junction is not limited to LSMO used previously, but is actually rather wide, including all half metals that are structurally and chemically compatible with the PZT barrier. Possible candidates [3] include half-metallic double perovskites, which might allow the effect to be observed also at room temperature.

It is also interesting to note that a significant enhancement of the barrier FE distortions, relative to the PZT FE displacements, tends to decouple the interfacial O from the Ti/Zr layer at the Co interface and reduce/suppress the spin filtering effect for $P_{\downarrow}$ (see Supplemental Material [30]). This may explain the absence of this effect in Co/$PbTiO_3$/LSMO MTJs [4].

IV. CONCLUSION

We present a first-principles study that reveals a possible mechanism for the experimentally observed FE switching of spin-polarization direction in the Co/PZT/LSMO MTJ. Starting from the ideal, chemically abrupt Co/PZT interface, we consider the effects of various types of defects and identify an atomic interface configuration that accounts for the experimental spin-polarization switching behavior. This configuration includes an O vacancy in the TZO_2 plane and an O atom placed in the interstitial position closest to the interface with Co. Oxygen vacancies are the most-often-encountered defects in oxides, and also commonly form at metal/oxide interfaces. Our *ab initio* calculations uncover a mechanism by which the interfacial O atom, through the PZT FE displacements, changes its reactivity and the strength of the chemical interaction with the Co plane, causing *on-off* switching of the O-Co hybridization. This process is responsible for the dynamical FE-induced spin-filtering effect that we observe in this study. In addition, the behavior of the probability density of the barrier states at E_F on switching of the FE polarization at the same interface is also consistent with the observed experimental FE resistive switching trend.

ACKNOWLEDGMENT

We acknowledge CINECA Award No. IsC10_MF-OXINT under the ISCRA initiative for the availability of high-performance computing resources and support.

[1] F. Matsukura, Y. Tokura, and H. Ohno, Control of magnetism by electric fields, Nat. Nanotechnol. **10**, 209 (2015).
[2] Julian P. Velev, Chun-Gang Duan, J. D. Burton, Alexander Smogunov, Manish K. Niranjan, Erio Tosatti, S. S. Jaswal, and Evgeny Y. Tsymbal, Magnetic tunnel junctions with ferroelectric barriers: Prediction of four resistance states from first principles, Nano. Lett. **9**, 427 (2009).
[3] D. Pantel, S. Goetze, D. Hesse, and M. Alexe, Reversible electrical switching of spin polarization in multiferroic junctions, Nat. Mater. **11**, 289 (2012).
[4] Andy Quindeau, Ignasi Fina, Xavi Marti, Geanina Apachitei, Pilar Ferrer, Chris Nicklin, Eckhard Pippel, Dietrich Hesse, and Marin Alexe, Four-state ferroelectric spin-valve, Sci. Rep. **5**, 09749 (2015).
[5] Hajo J. A. Molegraaf, Jason Hoffman, Carlos A. F. Vaz, Stefano Gariglio, Dirk van derMarel, Charles H. Ahn, and

Jean-Marc Triscone, Magnetoelectric effects in complex oxides with competing ground states, Adv. Mater. **21**, 3470 (2009).

[6] Lu Jiang, Woo Seok Choi, Hyoungjeen Jeen, Shuai Dong, Yunseok Kim, Myung-Geun Han, Yimei Zhu, Sergei V. Kalinin, Elbio Dagotto, Takeshi Egami, and Ho Nyung Lee, Tunneling electroresistance induced by interfacial phase transitions in ultrathin oxide heterostructures, Nano Lett. **13**, 5837 (2013).

[7] R. Ramesh, Ferroelectrics: A new spin on spintronics, Nature Mater. **9**, 380 (2010).

[8] V. Garcia, M. Bibes, L. Bocher, S. Valencia, F. Kronast, A. Crassous, X. Moya, S. Enouz-Vedrenne, A. Gloter, D. Imhoff, C. Deranlot, N. D. Mathur, S. Fusil, K. Bouzehouane, and A. Barthélemy, Ferroelectric control of spin polarization, Science **327**, 1106 (2010).

[9] V. S. Borisov, S. Ostanin, I. V. Maznichenko, A. Ernst, and I. Mertig, Magnetoelectric properties of the $Co/PbZr_xTi_{1-x}O_3(001)$ interface studied from first principles, Phys. Rev. B **89**, 054436 (2014).

[10] Vladislav S. Borisov, Sergey Ostanin, Steven Achilles, Jürgen Henk, and Ingrid Mertig, Spin-dependent transport in a multiferroic tunnel junction: Theory for $Co/PbTiO_3/Co$, Phys. Rev. B **92**, 075137-9 (2015), note and references therein.).

[11] O. Vlašín, R. Jarrier, R. Arras, L. Calmels, B. Warot-Fonrose, C. Marcelot, M. Jamet, P. Ohresser, F. Scheurer, R. Hertel, G. Herranz, and S. Cherifi-Hertel, Interface magnetoelectric coupling in $Co/Pb(Zr, Ti)O_3$, ACS Appl. Mater. Interfaces **8**, 7553 (2016).

[12] M. Imam, N. Stojić, and N. Binggeli, Ferroelectric switching of band alignments in LSMO/PZT/Co multiferroic tunnel junctions: An ab initio study, Nanotechnology **28**, 315202 (2017).

[13] For the defect-free interfaces with the various layer terminations the trend is always opposite, namely the spin polarization becomes negative or increasingly negative when the FE-polarization is changed from pointing towards Co to pointing against Co [9–12].

[14] G. Holzlechner, D. Kastner, C. Slouka, H. Hutter, and J. Fleig, Oxygen vacancy redistribution in $PbZr_xTi_{1-x}O_3$ (PZT) under the influence of an electric field, Solid State Ion. **262**, 625 (2014).

[15] Feng Chen, Robert Schafranek, Wenbin Wu, and Andreas Klein, Reduction-induced Fermi level pinning at the interfaces between $Pb(Zr, Ti)O_3$ and Pt, Cu and Ag metal electrodes, J. Phys. D Appl. Phys. **44**, 255301 (2011).

[16] C. Ma, B. Ma, S.-B. Mi, M. Liu, and J. Wu, Enhanced dielectric nonlinearity in epitaxial $Pb_{0.92}La_{0.08}Zr_{0.52}Ti_{0.48}O_3$ thin films, Appl. Phys. Lett. **104**, 162902-5 (2014).

[17] S. Gottschalk, H. Hahn, S. Flege, and A. G. Balogh, Oxygen vacancy kinetics in ferroelectric $PbZr_{0.4}Ti_{0.6}O_3$, J. Appl. Phys. **104**, 114106-7 (2008).

[18] R.-V. Wang and P. C. McIntyre, ^{18}O tracer diffusion in $Pb(Zr, Ti)O_3$ thin films: A probe of local oxygen vacancy concentration, J. Appl. Phys. **97**, 023508-8 (2005).

[19] P. Giannozzi, *et al.*, Quantum espresso: A modular and open-source software project for quantum simulations of materials, J. Phys.: Condens. Matter **21**, 395502 (2009).

[20] D. Vanderbilt, Soft self-consistent pseudopotentials in a generalized eigenvalue formalism, Phys. Rev. B **41**, 7892 (1990).

[21] The pseudopotentials used and their configurations are the same as in our previous study in Ref. [12].

[22] L. Bellaiche and David Vanderbilt, Virtual crystal approximation revisited: Application to dielectric and piezoelectric properties of perovskites, Phys. Rev. B **61**, 7877 (2000).

[23] I. I. Oleinik, E. Y. Tsymbal, and D. G. Pettifor, Atomic and electronic structure of $Co/SrTiO_3/Co$ magnetic tunnel junctions, Phys. Rev. B **65**, 020401-4 (2001).

[24] B. Zheng and N. Binggeli, Effects of chemical order and atomic relaxation on the electronic and magnetic properties of $La_{2/3}Sr_{1/3}MnO_3$, J. Phys.: Condens. Matter **21**, 115602 (2009).

[25] We also compare the LDOS in the Co/PZT-interface regions obtained for the Co/PZT bilayer and Co/PZT/LSMO trilayer with abrupt Co/PZT interfaces and PZT-slab thickness of seven PZT unit cells with the same three frozen PZT unit cells. The resulting LDOS in the interfacial region are virtually identical (for both $P_\downarrow$ and $P_\uparrow$).

[26] M. Peressi, N. Binggeli, and A. Baldereschi, Band engineering at interfaces: Theory and numerical experiments, J. Phys. D: Appl. Phys. **31**, 1273 (1998).

[27] M. Stengel, P. A. Puente, N. A. Spaldin, and J. Junquera, Band alignment at metal/ferroelectric interfaces: Insights and artifacts from first principles, Phys. Rev. B **83**, 235112 (2011).

[28] Pablo Aguado-Puente and Javier Junquera, First-principles study of metal-induced gap states in metal/oxide interfaces and their relation with the complex band structure, MRS Commun. **3**, 191 (2013).

[29] X. G. Zhang and W. H. Butler, Band structure, evanescent states, and transport in spin tunnel junctions, J. Phys. Cond. Matter **15**, R1603 (2003).

[30] See Supplemental Material at http://link.aps.org/supplemental/10.1103/PhysRevApplied.11.014028 for more information on effective spin polarization.

[31] The atomic positions at the interface are optimized for each configuration.

[32] Not being able to explain the observed experimental spin-polarization switching trend with the defect-free Co/PZT interface, we considered also the higher-energy interfacial structures that could appear experimentally for kinetic reasons.

[33] Consistent with the LDOS at and near E_F shown in the inset in Fig. 2 and in Fig. 3.

[34] The TMR ratio [3] within the Julliere generalized model is $\mathrm{TMR} = (2P_s(1)P_s(2)/(1 - P_s(1)P_s(2))$, where $P_s(1)$ and $P_s(2)$ are the spin-polarization values of the transmission probabilities from the two interfaces of the barrier. We take into account the half-metal nature of LSMO with $P_s(1) = 1$ and measure $P_s(2)$ from the spin polarization of $\rho(E_F, z)$ well within PZT.

[35] To check that the electric field present in the vacuum due to an asymmetric Co/PZT(001)-slab configuration does not play an important role, we optimize the atomic structure also in the case without a field in a supercell consisting of the Co/PZT/Co trilayer containing simultaneously the $P^\uparrow$ and $P^\downarrow$ polarizations at the two interfaces. The relative

Co/PZT-interface relaxations are identical to those in the case of bilayer calculations for both FE polarizations.

[36] From the Julliere model, we obtain TMR ratios of -5 for $P_{\uparrow}$ and 22% for $P_{\downarrow}$ at the second PbO layer from the PZT/Co interface. The TMR values have the same sign as the measured ratios (while the TMR values of the ideal defect-free interface are -25% for $P_{\uparrow}$ and -59% for $P_{\downarrow}$ at the combined first PZT layer at the PZT/Co interface).

[37] The interface O atom is significantly magnetic, with 0.26 μ_B for $P^{\downarrow}$, while for $P^{\uparrow}$ the magnetic moment is much smaller, 0.11 μ_B. The Ti atom for $P^{\downarrow}$ is aligned antiferromagnetically with O and Co, with a moment of $-0.05\,\mu_B$, and for $P^{\uparrow}$ its moment is only 0.01 μ_B.

[38] E. Y. Tsymbal and D. G. Pettifor, Modelling of spin-polarized electron tunnelling from 3d ferromagnets, J. Phys.: Cond. Matter **9**, L411 (1997).

[39] D. Nguyen-Manh, E. Y. Tsymbal, D. G. Pettifor, C. Arcangeli, R. Tank, O. K. Andersen, and A. Pasturel, Spin-polarized density of states and electron tunnelling from the Co/Al_2O_3 interface, Mat. Res. Soc. Symp. Proc. **492**, 319 (1997).

[40] J. M. De Teresa, A. Barthélémy, A. Fert, J. P. Contour, R. Lyonnet, F. Montaigne, P. Seneor, and A. Vaurès, Inverse Tunnel Magnetoresistance in $Co/SrTiO_3/La_{0.7}Sr_{0.3}MnO_3$: New Ideas on Spin-Polarized Tunneling, Phys. Rev. Lett. **82**, 4288 (1999).

[41] E. Y. Tsymbal, K. D. Belashchenko, J. P. Velev, S. S. Jaswal, M. van Schilfgaarde, I. I. Oleynik, and D. A. Stewart, Interface effects in spin-dependent tunneling, Prog. Matter. Sci. **52**, 401 (2007).

[42] M. Fechner, I. V. Maznichenko, S. Ostanin, A. Ernst, J. Henk, P. Bruno, and I. Mertig, Magnetic phase transition in two-phase multiferroics predicted from first principles, Phys. Rev. B **78**, 212406-4 (2008).

[43] G. Radaelli, D. Petti, E. Plekhanov, I. Fina, P. Torelli, B. R. Salles, M. Cantoni, C. Rinaldi, D. Gutiérrez, G. Panaccione, M. Varela, S. Picozzi, J. Fontcuberta, and R. Bertaccoa, Electric control of magnetism at the $Fe/BaTiO_3$ interface, Nat. Commun. **5**, 3404 (2014).

[44] Julian P. Velev, Juan M. López-Encarnación, J. D. Burton, and Evgeny Y. Tsymbal, Multiferroic tunnel junctions with poly(vinylidene fluoride), Phys. Rev. B **85**, 125103 (2012).

Correction: The title was not updated properly and has been fixed.